Genetic-algorithm implementation of atomic potential reconstruction from differential electron scattering cross sections

Junliang Xu,[1,*] Hsiao-Ling Zhou,[2] Zhangjin Chen,[1] and C. D. Lin[1]

[1]*Department of Physics, Cardwell Hall, Kansas State University, Manhattan, Kansas 66506, USA*
[2]*Department of Physics and Astronomy, Georgia State University, Atlanta, Georgia 30303, USA*

We demonstrate the successful implementation of genetic algorithm for the retrieval of atomic potentials using elastic differential cross sections (DCSs) between free electrons and atomic ions for electron energies from a few to several tens of electron volts. Since the DCSs over this energy region can be extracted from laser-generated high-energy photoelectron momentum spectra, the results suggest that infrared lasers can be used to image the target structure. Extending to molecular targets, in particular, to transient molecules created by an earlier pump pulse, our results suggest that few-cycle infrared probe lasers can be used for dynamic chemical imaging with temporal resolution of a few femtoseconds.

I. INTRODUCTION

When an object is illuminated by a plane wave, the amplitude of the diffraction pattern in the far field is the Fourier transform of the object [1]. To achieve high spatial resolution, x rays or electrons with energies on the order of tens to hundreds of keV are used. These are powerful tools for spatial imaging of the structure at the atomic level, but they are not suitable for transient molecules which vary in a few to hundreds of femtoseconds. To achieve such temporal resolution, new technology such as x-ray free-electron lasers (XFELs) and ultrafast electron-diffraction (UED) [2] technologies are being developed.

Today infrared laser pulses with duration of a few femtoseconds are widely accessible. However, these lasers have wavelength much longer than the interatomic distances. Hence they are considered not suitable for imaging ultrafast structural changes in molecules. Nevertheless, the possibility of using infrared lasers for imaging molecules from laser-induced electron-diffraction spectra has been proposed more than a decade ago [3]. Similarly, high-order harmonics generated by infrared lasers have also been proposed for probing the structure of the target [4–6]. The underlying reason for the possibility is best understood using the well-known rescattering model. When an atom or molecule is placed in a laser field, electrons which are released by tunneling ionization in the early part of the laser field may be driven back and accelerated by the laser when its electric field changes direction. The returning electrons may revisit the target where they may be backscattered elastically by the ion, or they may recombine with the ion to emit high-energy photons. Since electron scattering and photoionization are the standard tools for probing the structure of atoms and molecules, thus in principle there is some information on the target structure that can be extracted from the emitted electrons or photons. Despite this optimism, however, few accurate structural information actually has emerged from laser-atom and laser-molecule interactions so far. This is not

unexpected since the role of target structure in the nonlinear interaction of lasers with atoms and molecules is still not understood at the quantitative level. In particular, prevailing theories such as tomographic method [4], two-center interference model [7], and improved strong-field approximation [8] all treat the continuum electrons by plane waves, thus leaving out the important interaction of electrons with the target. Thus, while these models have stimulated the interest in the field, progress in dynamic chemical imaging is possible only after the interaction between electron and the target ion is properly treated.

Recently we have developed a quantitative rescattering (QRS) theory [9–11] for laser-induced high-energy photoelectron momentum spectra. Using the photoelectron momentum spectra calculated from solving the time-dependent Schrödinger equation as well as from experimental data, we showed that accurate elastic differential cross sections (DCSs) between free electrons and rare-gas target ions can be extracted. The DCSs thus obtained are in good agreement with the DCS calculated from electron-ion collision theories, and in one case, in agreement with experimental data taken from electron collisions with Ar^+ ions [12]. In future experiments, we assume that DCS can be obtained from the measured photoelectron spectra. In this paper, we ask whether one can extract accurate target structure information from such DCSs. Since the energies of the returning electrons are on the order of tens of electron volts only, the standard diffraction theory where the continuum electrons are approximated as plane waves cannot be used. Instead scattering waves should be used. In this paper we report the result of such an attempt.

The problem of constructing the interaction potential between two colliding particles from scattering data or from the spectroscopy data from the bound systems has been extensively investigated in the past half a decade. In particular, using elastic differential scattering cross sections from molecular-beam experiments [13], atom-atom or atom-diatom interatomic potentials have been extracted [14]. The most common approaches rely on either a phenomenological potential parameter fitting [15] or an iterative perturbation method [16]. More recently, Rabitz and co-workers [17] de-

───────
*junliang@phys.ksu.edu

veloped a global, noniterative algorithm for inverting the quantum scattering observations to obtain intermolecular potentials.

Quantum-mechanical inverse scattering problems are not as well investigated in atomic systems. Amos and co-workers [18] extracted the spin-orbit interaction from elastic-scattering cross sections at 5 eV between electrons with Xe atoms. No such investigations have been carried out for the collision between electrons with atomic ions. However, the spectra of neutral atoms have been widely used to derive an approximate central local potential $V(r)$, where r is the distance of the active electron from the atomic nucleus. Such a model potential approach is useful most often when the atoms are investigated in an external field or involved in collisions with other particles. The model potential is parametrized in some analytic form, and the parameters are chosen such that bound-state energies calculated from the potential $V(r)$ are closed to experimental values.

In this paper we aim at finding a robust inversion method which can be used to obtain accurate model potentials for rare-gas atoms based on the differential elastic-scattering cross sections. Specifically, we assume that experimental elastic differential cross sections are available for large scattering angles with incident electron energies in the range of about 2.0–50 eV. The targets are Ne$^+$, Ar$^+$, Kr$^+$, and Xe$^+$ ions. For the inversion method, we used the genetic algorithm (GA). Without imposing much "prior" knowledge about the target, we show that a retrieval of the atomic target potential $V(r)$ is possible.

The rest of this paper is arranged as the following. For completeness, we first explain in Sec. II how GA functions and how the DCSs are calculated quantum mechanically if a central potential $V(r)$ is given. In Sec. III, we used a model potential of Ar to generate the DCS, and then used GA to retrieve this potential. This method is shown to work for the model Ar, Ne, Kr, and Xe atoms. In Sec. IV we used DCSs calculated with R-matrix (RMAT) approach as "experimental data." We assume random errors of no more than 10% and angular resolution of 5° and only the relative cross sections are known. Using GA we are able to obtain the potentials $V(r)$ for Ne, Ar, and Kr. For Xe, the potential which gives the best fit of the cross sections turns out to be incorrect, but the next better-fit one is correct. In Sec. V we sum up our GA-fitting experience. A short summary and discussion of extending this work for dynamic chemical imaging with infrared lasers are given in Sec. VI. Atomic units are used in this paper unless otherwise indicated.

II. GENETIC ALGORITHM AND THE CALCULATION OF ELASTIC DIFFERENTIAL SCATTERING CROSS SECTION

A. Statement of the problem

Suppose elastic differential scattering cross sections $\sigma_e(k, \theta)$ have been obtained between an incident electron and a singly charged atomic ion, over a range of electron momentum and scattering angles experimentally. We wish to construct a spherically symmetric model potential $V(r)$ which will reproduce the DCSs as close to $\sigma_e(k, \theta)$ as pos-

sible. Since the range of k and θ will be limited, it will not be treated as a standard inverse scattering problem. Instead, we seek the solution by using GA. The potential will be parametrized in the form

$$V(r;\boldsymbol{a}) = -\frac{1 + a_1 e^{-a_2 r} + a_3 r e^{-a_4 r} + a_5 e^{-a_6 r}}{r}. \tag{1}$$

Since we are treating neutral atoms, the asymptotic charge in Eq. (1) has been set to 1.0. We assume that we do not know the target, but for small r, the target nucleus charge is related to the coefficients $\{a_i\}$ by $Z = 1 + a_1 + a_5$. Note that in this model, we treat the atom using single-active-electron approximation. Rare-gas atoms will be used for this test.

The parameter set $\boldsymbol{a} = \{a_1, a_2, a_3, a_4, a_5, a_6\}$ forms a six-dimensional search space. For each known possible solution $\boldsymbol{a}$, which is called an individual in GA, we first calculate the DCS $\sigma(k, \theta; \boldsymbol{a})$ for the scattering by the potential $V(r; \boldsymbol{a})$. The fitness of this individual is then calculated from a fitness or objective function

$$\chi^2(\boldsymbol{a}) = \sum_{i,j} k_i^4 [\sigma(k_i, \theta_j; \boldsymbol{a}) - \sigma_e(k_i, \theta_j)]^2. \tag{2}$$

Note that we use weighted DCS $k^2\sigma$ in order to give more or less equal weight to the DCS at different energies. Obviously individuals with lower fitness values are considered better designs, and we aim to find a parameter set $\boldsymbol{a} = \{a_i\}$ with possibly lowest fitness using GA.

We comment that the model potential approach for the DCS calculation used here neglects the electron exchange, core polarization, and other many-electron correlation effects. This approximation is adequate for electron scattering for energies above 10 eV and more. The DCS calculated from model potential method are in good agreement with those from the R-matrix calculations, see Sec. II C.

B. Genetic algorithm

In this work we used the GA driver GA v1.7a, implemented by Carroll [19] and written in FORTRAN language. In this code, binary encoding of the parameter set $\{a_i\}$ is adopted. Both simple genetic algorithm (SGA) and micro-genetic algorithm (micro-GA) can be used. We use micro-GA in this work. Similar to SGA [20], two operators are employed in micro-GA: (parent) selection and crossover. Both GAs start with an initial population, i.e., a group of candidate parameter sets, which are randomly selected from the search space. Next, the fitness of each individual is evaluated, which identifies their survival ability.

In the following evolutionary process, to create offspring for the next generation which will totally replace the current population, parents are selected according to their fitness. In other words, the fitter individuals will be emphasized more in hope that in turn they will have offspring with even lower fitness. The selection scheme applied in the work is tournament selection with tourney size 2. In this scheme, two candidate individuals will be randomly chosen with shuffling technique. The fitter will then win out to be one mate; the other mate will be fixed by running another tournament.

Afterward, marriage of all pairs of mates will generate the new generation, whose genetic construction descends from their parents' by crossover. It is worthy of pointing out again that crossover is performed on the basis of binary encodings instead of real-valued encodings. In more detail, each individual, an ordered list of the six real-valued parameters in each set, will be encoded into a binary sequence with each bit representing a "gene". In this study, uniform crossover is adopted in which gene exchange happens at each bit locus with probability p_{cross}. Elitism is also applied which simply retains the current best-fit individual in the next generation, in case that it may be destroyed by crossover. GA practice tells us elitism could efficiently cover against the negativeness of crossover and significantly improve the GA's performance. Different from SGA, micro-GA does not perform mutation operation on the offspring.

Once the next generation is created, a new round of evolution procedure starts over again. This loops until the maximum number of generations, G_{max}, set previously is reached and ends with output of the best parameter set found by then.

Besides the difference in mutation from SGA, micro-GA evolves only a small population (typically population size N_{pop} is 4–10), which will largely cut down the number of fitness-function evaluations and the computer time. Nevertheless, genetic diversity is not able to be maintained for many generations if "the population evolves in normal GA fashion" [19]. To prevent premature convergence, similarity of the whole population is checked for every generation. The genes of the best individual in each generation will be compared with those of the rest of the population locus by locus. If the variability, defined as the weight of the nonidentical bits out of the total bits, is less 5%, the micro-GA will restart with the best individual and randomize the others.

C. Calculation of differential elastic-scattering cross sections

Since the fitness function is based on the elastic DCS, we describe briefly how the DCS is calculated for each candidate potential $V(r; \boldsymbol{a})$. First, we separate out the long-range Coulomb potential, such that

$$V(r) = -\frac{1}{r} + V_S(r), \qquad (3)$$

in which $V_S(r)$ is the short-range potential. In standard quantum-mechanics textbooks, $V(r)$ is called a modified Coulomb potential. The total differential scattering amplitude for such a potential can be written as

$$f(\theta) = f_c(\theta) + f_S(\theta), \qquad (4)$$

where $f_c(\theta)$ is the Coulomb scattering amplitude,

$$f_c(\theta) = -\frac{\eta}{2k \sin^2\frac{\theta}{2}} e^{-i\{\eta \ln[\sin^2(\theta/2)] - 2\sigma_0\}}, \qquad (5)$$

with $\eta = -1/k$ and $\sigma_0 = \arg[\Gamma(1 + i\eta)]$. The scattering amplitude f_S from the short-range potential $V_S(r)$ is given by

$$f_S(\theta) = \sum_{l=0}^{\infty} \frac{2l+1}{k} e^{2i\sigma_l} e^{i\delta_l} \sin \delta_l P_l(\cos \theta), \qquad (6)$$

where the Coulomb phase shift for each partial wave is

$$\sigma_l = \arg[\Gamma(l + 1 + i\eta)] \qquad (7)$$

and δ_l is the phase shift from the short-range potential.

For the present purpose, we do not have experimental DCS, $\sigma_e(k, \theta)$. Thus we generate the experimental data in two ways. One is to start with a given model potential for a given atom to generate the DCS. We then use the GA, and see if we can recover this potential. Alternatively, we can use the R-matrix method [21] to calculate the DCS. In the R-matrix method, the target states are expressed as configuration-interaction expansion of Hartree-Fock orbitals. The resulting close-coupling equations for the continuum electron are solved with the R-matrix method. Note that in RMAT calculation, all the electrons in the atom are considered, i.e., not in the single-active-electron approximation.

D. GA parameters and restrictions on the potential parameters

This is an indirect fitting procedure. We want to construct the potential $V(r; \boldsymbol{a})$ by best fitting the elastic DCS. In sum, there are four GA parameters: population size N_{pop}, crossover rate p_{cross}, maximum number of generations G_{max}, and initial random number seed i_{seed} which is negative to warm up the random number generator. The computer time mainly depends on the total number of fitness evaluations which is proportional to N_{pop} and G_{max}. Generally speaking, smaller population size will make the GA run faster and yet evolution flow converges slower. On the other hand, larger G_{max} surely lowers the risk of getting a nonconverged best fit but will linearly increase the computer time. Thus we balance computer time and GA convergence, but give the priority to the latter. For micro-GA, $p_{cross} = 0.5$ is appropriate for uniform crossover and we prefer $N_{pop} = 5$–6. We set G_{max} as a number as large as possible within the limit of computer time that we are willing to accept. Using micro-GA, the computer time is shorter, but at the expense of slower evolution convergence. Another way to reduce computer time is to put some restrictions on the potential parameters. For example, the nuclear charge Z should be between 1 and 118, and the effective charge $Z_{eff}(r; \boldsymbol{a}) = -rV(r; \boldsymbol{a}) > 0$ should be a decreasing function of radius r, i.e., $Z'_{eff}(r; \boldsymbol{a}) < 0$. For the parameter sets $\boldsymbol{a}$ which do not satisfy these conditions, there is no need to further calculate the DCS. We simply set a very large fitness value for them. Note that the inverse problem does not guarantee a unique solution in general. This is also true for GA. These additional constraints are useful for helping to sort out the acceptable solutions.

III. GA FITTING WITH ELASTIC DCS GENERATED FROM A GIVEN MODEL POTENTIAL

In this first test, we feed the DCS generated from a known potential $V(r)$. The range of k is taken to be [0.3,2.0] with 21 equal-spaced grid points. The scattering angle θ runs from
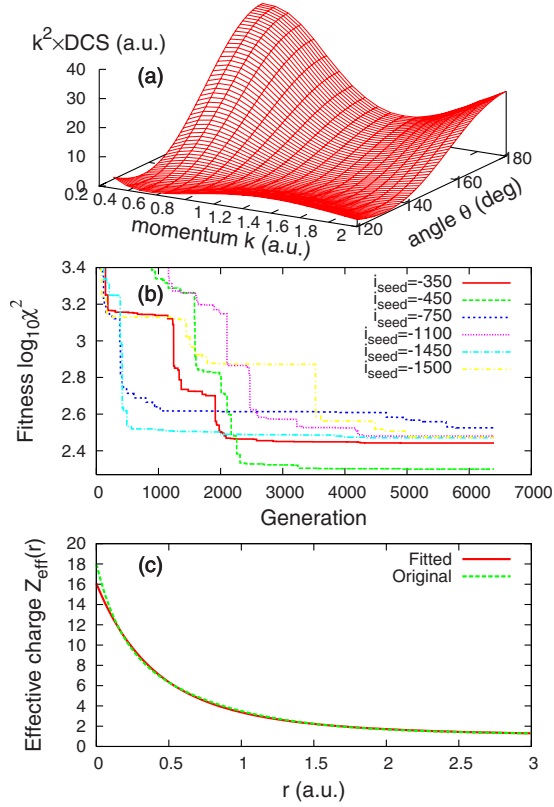
FIG. 1. (Color online) (a) Weighted elastic DCSs of Ar fed into the micro-GA, for momenta $k \in [0.3, 2.0]$ and angles $\theta \in [120°, 180°]$. (b) Evolution of the best fitness per generation associated with different random number generator seeds i_{seed}. (c) Comparison of the fitted and the original effective charges $Z_{eff}(r)$.

120° to 180° with an increment of 1°. The GA parameters are set up with $N_{pop}=6$ and $G_{max}=6400$. We chose Ar for this test, using the model potential from [22]. In Fig. 1(a) the "experimental" DCS surface is shown (note that the DCS is weighted by k^2). In the test, we set i_{seed} to a series of numbers from −50 to −1500 in steps of 50, which results in assorted curves in Fig. 1(b), ending with different fitness values at generation $G_{max}=6400$. Note that only six curves with the lowest fitness are shown in Fig. 1(b) for clarity. However, it is difficult to draw a simple rule about the final behavior of fitness curves with different i_{seed}, as two vicinal seeds could have the fitness scattered far away from each other at the end, and vice versa. It is therefore fair to say that GA outcomes are "randomly" distributed. In this study, 30 seeds, i.e., 30 independent runs, are deemed capable of providing a reasonably good fit.

The fitted potential from this test run is shown in Fig. 1(c), which is compared to the input potential. Good agreement between the two can be seen. The ratio of the error is less than 4% over all range of r except near the origin where the error is 10%. Nevertheless, from GA, we obtained $1 + a_1 + a_5 = 16.1$, which is close to $Z=18$ for Ar.

In Fig. 1 the experimental data were selected for the region of $k=[0.3, 2.0]$. Since low-energy electrons do not penetrate near the nucleus, this may explain why the retrieved potential there is not as accurate as we like it to be. We next used experimental data for $k=[2.0, 3.0]$. The DCS surface in
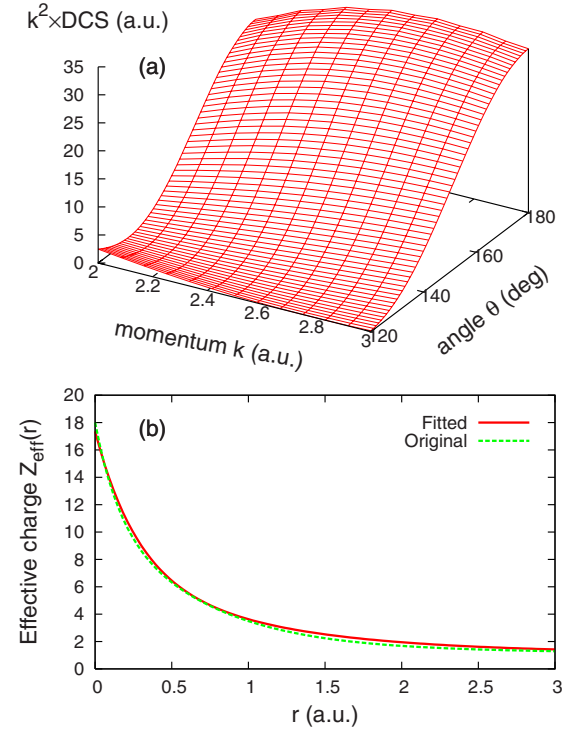
FIG. 2. (Color online) (a) Weighted DCSs of Ar for $k \in [2.0, 3.0]$ and $\theta \in [120°, 180°]$. (b) Comparison of the fitted and the original effective charges $Z_{eff}(r)$.

this range is shown in Fig. 2(a). The potential obtained from GA is compared to the input potential in Fig. 2(b). We can see clear improvement in the agreement in the small-r region. The nuclear charge calculated from $1 + a_1 + a_5 = 17.35$ is now close to $Z=18$ used in the input.

We have tested GA for other rare-gas atoms such as Ne, Kr, and Xe, and similar results have been obtained. As an example, the experimental DCSs for Xe are shown in Fig. 3(a) and the retrieved potential is shown in Fig. 3(b), which is in good agreement with the input potential.

IV. GA FITTING WITH ELASTIC DCS GENERATED FROM *R*-MATRIX CALCULATION

In this section, we will use the elastic DCS calculated with RMAT method as experimental data. Differently from Sec. III, in RMAT calculations no input potential is available and all the electrons are considered in the DCS calculation. To make the simulation more "realistic", we assume that experimentally only the relative DCSs are provided. Thus we arbitrarily multiply the calculated DCS by a factor of 10. We further introduce "experimental" errors of no more than 10% using a random number generator and "instrumental" angular resolution $\Delta\theta=5°$ on the data. The angular range is taken between 100° and 180° and k is chosen in the range of [0.4, 2.0] at 21 equally spaced points.

Because the theory calculates absolute DCS, while the experiment gives only the relative values, the fitness function now is modified to

$$\chi^2(\boldsymbol{a}) = \sum_{i,j} k_i^4 [f\sigma(k_i, \theta_j; \boldsymbol{a}) - \sigma_e(k_i, \theta_j)]^2. \quad (8)$$
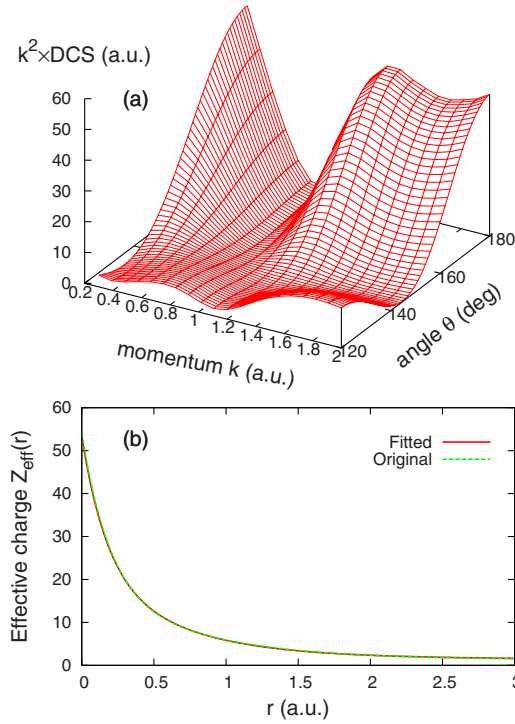
FIG. 3. (Color online) (a) Weighted DCSs of Xe for $k \in [0.3, 2.0]$ and $\theta \in [120°, 180°]$. (b) Comparison of the fitted and the original effective charges $Z_{eff}(r)$.

The factor f is determined by

$$f = \frac{\sum\limits_{i,j} k_i^4 \sigma(k_i, \theta_j; \boldsymbol{a}) \sigma_e(k_i, \theta_j)}{\sum\limits_{i,j} k_i^4 [\sigma(k_i, \theta_j; \boldsymbol{a})]^2}, \qquad (9)$$

which corresponds to the minimum of $\chi^2(\boldsymbol{a})$ in Eq. (8).

In Fig. 4 the DCS surfaces for Kr, Ar, and Ne obtained from the RMAT calculations are shown. They actually are quite close to those generated from model potentials used in Sec. III (but we assume that is not known). With GA setup of $N_{pop}=5$ and $G_{max}=6400$, the fitting process went through very smoothly, and the fitted model potentials are given in Fig. 5. In this figure, we also show the model potentials obtained from [22]. Note that for the latter, the model potential is fitted with the energy of the ground state as well as a few excited states. From GA, the extracted nuclear charges are 9.5, 16.7, and 35.2, for Ne, Ar, and Kr, respectively. As noted earlier, more accurate nuclear charges can be obtained if DCSs at higher energies are used.

Without the $V(r)$ to check the accuracy, one can compare the energy levels calculated from the retrieved $V(r)$ with experimental data. This is shown in Table I. We note that the agreement is acceptable. For the excited states, the error is typically better than 5%, with larger error for the ground state. The larger error for the ground state is not surprising. To begin with, we already know that the potential near the nucleus is not as well retrieved using the set of experimental DCS data in this simulation. Furthermore, the fitness function is for the DCS only.
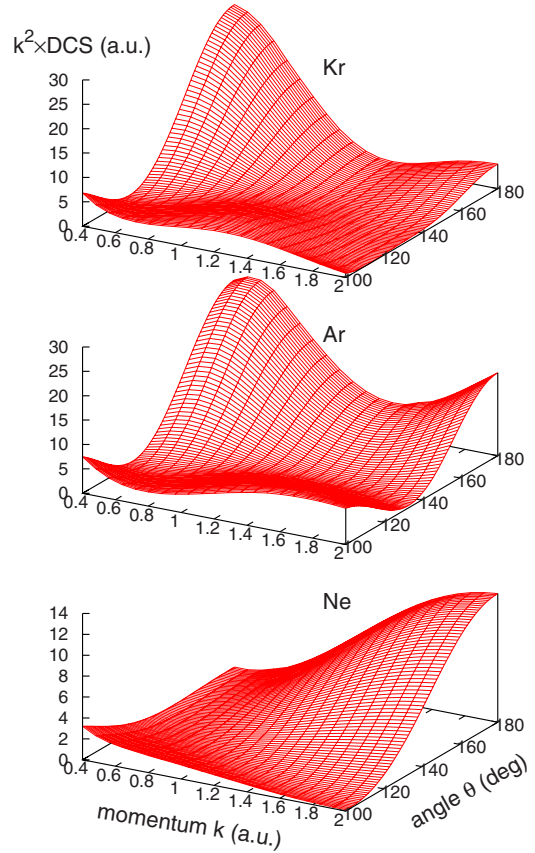
FIG. 4. (Color online) Weighted DCSs calculated with RMAT method for Ne, Ar, and Kr for momenta $k \in [0.4, 2.0]$ and angles $\theta \in [100°, 180°]$.

Despite the success shown above, one should not come away with the impression that GA always works so well. Using the DCS calculated from RMAT approach for Xe, as shown in Fig. 6(a), we retrieved the effective charge $Z_{eff}(r)$, showing results from the two with the best fitness. It is clear that the one with the best fitness is incorrect since it would give a nuclear charge close to 90. The second best fit actually results in model potential that is closer to the correct answer. See additional comments below.

V. GA-FITTING EXPERIENCE

Inverse scattering problem is a very large subject. In principle, many multiparameter optimization techniques could be applicable and GA is only one of them. As we have found above, the search space for our problem is large, and the landscape is not known well enough and complicated, containing many valleys [see, e.g., Fig. 1(b)]. The fitness function is not perfectly smooth due to restrictions on the fitting parameters. Research has shown that GA is a good method to try for such problems [20].

The results shown above also confirm positive performance of GA for the present problem. For better understanding of micro-GA and also for completeness, the experience of these preliminary tests is briefly summarized here.

Convergence. To guarantee the convergence of the opti-
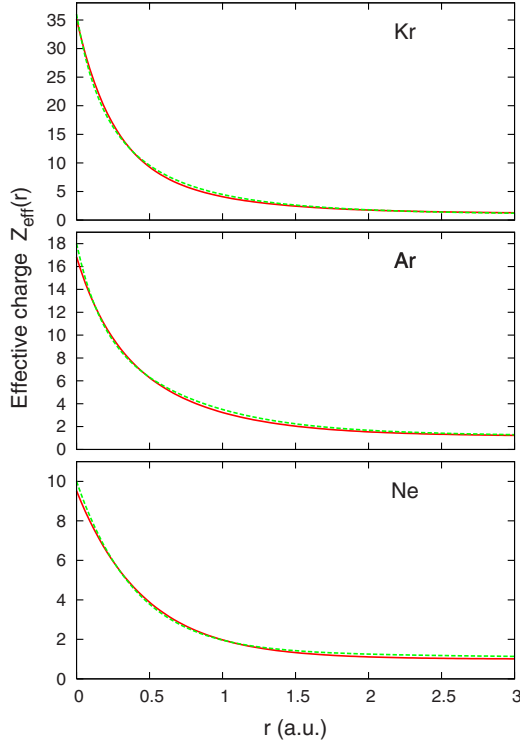
FIG. 5. (Color online) Fitted effective charges $Z_{eff}(r)$ (solid line) by using the data shown in Fig. 4 for Ne, Ar, and Kr. For comparison, effective charges (dashed line) from the model potentials in [22] are also plotted.

TABLE I. Comparison of the energy levels (in a.u.) from experiments and from the fitted potentials for Ne, Ar, and Kr. Error ratios are also shown as percentages.

	Configuration	Expt.[a]	GA
Ne	$2s^2 2p^6$	−0.792482	−0.832242 (5.02%)
	$2s^2 2p^5 3s$	−0.178868	−0.170281 (4.80%)
	$2s^2 2p^5 3p$	−0.108140	−0.106876 (1.17%)
	$2s^2 2p^5 4s$	−0.068261	−0.067332 (1.36%)
	$2s^2 2p^5 4p$	−0.048987	−0.049522 (1.09%)
	$2s^2 2p^5 5s$	−0.035578	−0.035754 (0.49%)
Ar	$3s^2 3p^6$	−0.579155	−0.467188 (19.33%)
	$3s^2 3p^5 4s$	−0.150964	−0.150609 (0.23%)
	$3s^2 3p^5 4p$	−0.095147	−0.098672 (3.70%)
	$3s^2 3p^5 5s$	−0.061856	−0.060740 (1.80%)
	$3s^2 3p^5 5p$	−0.043744	−0.045780 (4.65%)
	$3s^2 3p^5 6s$	−0.033707	−0.032724 (2.92%)
Kr	$4s^2 4p^6$	−0.514476	−0.464244 (9.76%)
	$4s^2 4p^5 5s$	−0.140347	−0.143238 (2.06%)
	$4s^2 4p^5 5p$	−0.093071	−0.092664 (0.44%)
	$4s^2 4p^5 6s$	−0.060086	−0.058833 (2.08%)
	$4s^2 4p^5 6p$	−0.044650	−0.044134 (1.16%)
	$4s^2 4p^5 7s$	−0.032900	−0.031910 (3.01%)

[a]Those are nonrelativistic levels roughly calculated by using term average.

mal parameter set in each evolution process, we suggested setting G_{max} as large as possible. However, the example of Xe in Fig. 6 tells us that one should check whether the best fits from different i_{seed} converge to each other or not. In the present work, this is performed by comparing their corresponding $Z_{eff}(r)$. In all the tests above, the convergence was confirmed.

Fitness function. As stated in Sec. II, a weight is needed to treat all the data sets more or less on equal footing in the fitness function. Since the DCS decreases with increasing kinetic energy of the electron, a weight of k^2 was multiplied to each DCS. Tests without a weight were also done but failed to come up with good fits.

Fine search. Local search may be mated with micro-GA to get a better design [23]. For a test, the multidimensional Nelder-Mead simplex search [24] was adopted which optimizes the best fit per generation by using it as the starting point. This turns out to be able to improve the final fit; e.g., Z of Ar in Fig. 1 could be improved to 17.5. However, the overall improvement is quite insignificant in view of the large increase in computer time. Thus local search was not adopted.

VI. SUMMARY AND OUTLOOK

In this paper the collision between an atomic ion with electrons is treated as the scattering of electrons from a model potential. By expressing the atomic potential in the form of Eq. (1) with six parameters, and assuming that elas-

FIG. 6. (Color online) (a) Weighted DCSs of Xe with the same range as in Fig. 4; (b) fitted effective charges $Z_{eff}(r)$. In (b), $Z_{eff}(r)$ of the two best fits are shown. Note that the best fit actually is incorrect. The second best fit agrees with the known model potential [22] well.

tic differential scattering cross sections are available "experimentally" over a range of energies and angles, we set to find the six parameters using the genetic algorithm. The input "experimental" data were obtained theoretically from another input potential, or from *R*-matrix calculations, assuming that only the relative cross sections are available and that there are in general a 10% intrinsic random errors and 5° angular resolution in the data. We found that the atomic potential retrieved using GA is quite accurate, as also evidenced by the fact that the retrieved potential reproduces experimental binding energies accurately. We emphasize that DCSs from backscattered electrons are used and electron energies of a few to a few tens of electron volts, as these are the typical returning electron energies when infrared lasers are used in laser-atom and laser-molecule interactions, in contrast to the standard electron-diffraction method where the electrons are in the hundreds of keV and the scattering angles are in the forward directions.

As indicated in Sec. I, our main goal is to retrieve structure of a transient molecule using high-energy above-threshold-ionization (HATI) electrons generated by few-cycle laser pulses where the laser duration is of a few femtoseconds [25]. According to the quantitative rescattering

theory we have recently developed, it is possible to extract accurate DCS from the momentum distributions of the HATI electrons. Using a pump laser to initiate a transition, the HATI electron momentum spectra can be measured with another few-cycle probe laser pulse. As shown by Chen *et al.* [11], for this purpose the phase stabilization of the laser pulse is not needed. Our next goal is to generate DCS from fixed-in-space molecules or molecules that are partially aligned or oriented and test the GA method to extract the structure of the molecule. Experimental HATI electron momentum spectra from isotropically [26] or partially aligned molecules [27] are beginning to emerge in many laboratories. The success of the method presented in this paper convinces us that GA may be used to retrieve the structure, i.e., the bond lengths and bond angles of a transient molecule, with temporal resolution of a few femtoseconds.

[1] J. Miao, C. Charalambous, H. Kirz, and D. Sayre, Nature (London) **400**, 342 (1999).

[2] H. Ihee, V. A. Lobastov, U. M. Gomez, B. M. Goodson, R. Srinivasan, C. Y. Ruan, and A. H. Zewail, Science **291**, 458 (2001).

[3] T. Zuo, A. D. Bandrauk, and P. B. Corkum, Chem. Phys. Lett. **259**, 313 (1996).

[4] J. Itatani, J. Levesque, D. Zeidler, H. Niikura, H. Pepen, J. C. Kieffer, P. B. Corkum, and D. M. Villeneuve, Nature (London) **432**, 867 (2004).

[5] V. H. Le, A. T. Le, R. H. Xie, and C. D. Lin, Phys. Rev. A **76**, 013414 (2007).

[6] V. H. Le, N. T. Ngugen, C. Jin, A. T. Le, and C. D. Lin, J. Phys. B **41**, 085603 (2008).

[7] M. Lein, J. Phys. B **40**, R135 (2007).

[8] D. B. Milošević, E. Hasović, M. Busuladžić, A. Gazibegović-Busuladžić, and W. Becker, Phys. Rev. A **76**, 053410 (2007).

[9] T. Morishita, A. T. Le, Z. Chen, and C. D. Lin, Phys. Rev. Lett. **100**, 013903 (2008).

[10] Z. Chen, A. T. Le, T. Morishita, and C. D. Lin, J. Phys. B **42**, 061001 (2009).

[11] Z. Chen, A. T. Le, T. Morishita, and C. D. Lin, Phys. Rev. A **79**, 033409 (2009).

[12] S. J. Brotton, P. McKenna, G. Gribakin, and I. D. Williams, Phys. Rev. A **66**, 062706 (2002).

[13] P. Casavecchia, G. He, R. K. Sparks, and Y. T. Lee, J. Chem. Phys. **75**, 710 (1981).

[14] U. Buck, Rev. Mod. Phys. **46**, 369 (1974); Comput. Phys. Rep. **5**, 1 (1986); D. R. Lun, K. Amos, and L. J. Allen, Phys. Rev. A **53**, 831 (1996); D. R. Lun, X. J. Chen, L. J. Allen, and K. Amos, *ibid.* **50**, 4025 (1994).

[15] G. R. Satchler, L. W. Owen, A. J. Elwyn, G. L. Morgan, and R. L. Watson, Nucl. Phys. A **112**, 1 (1986).

[16] A. A. Ioannides and R. S. Mackintosh, Nucl. Phys. A **467**, 482 (1987).

[17] J. M. Geremia and H. Rabitz, Phys. Rev. A **64**, 022710 (2001); T. Ho and H. Rabitz, J. Chem. Phys. **90**, 1519 (1989); R. Boyd *et al.*, *ibid.* **106**, 6548 (1997).

[18] A. Lovell and K. Amos, Phys. Rev. A **63**, 012707 (2000); D. R. Lun, M. Eberspächer, K. Amos, W. Scheid, and S. J. Buckman, *ibid.* **58**, 4993 (1998).

[19] D. L. Carroll, FORTRAN genetic algorithm driver, 1999, http://cuaerospace.com/carroll/ga.html (accessed in May 2008); in *Developments in Theoretical and Applied Mechanics XVIII*, edited by H. Wilson, R. Batra, C. Bert, A. Davis, R. Schapery, D. Stewart, and F. Swinson (School of Engineering, The University of Alabama, Tuscaloosa, 1996), pp. 411–424.

[20] D. E. Goldberg, *Genetic Algorithms in Search, Optimization & Machine Learning* (Addison-Wesley, Reading, MA, 1989); M. Mitchell, *An Introduction to Genetic Algorithms* (MIT Press, Cambridge, MA, 1996).

[21] K. A. Berrington, W. B. Eissner, and P. H. Norrington, Comput. Phys. Commun. **92**, 290 (1995).

[22] X. M. Tong and C. D. Lin, J. Phys. B **38**, 2593 (2005).

[23] J. M. C. Marques *et al.*, J. Phys. B **41**, 085103 (2008).

[24] W. H. Press *et al.*, *Numerical Recipes: The Art of Scientific Computing* (FORTRAN Version) (Cambridge University Press, New York, NY, 1992).

[25] T. Morishita, A. T. Le, Z. Chen, and C. D. Lin, New J. Phys. **10**, 025011 (2008).

[26] M. Okunishi, R. Itaya, K. Shimada, G. Prümper, K. Ueda, M. Busuladžić, A. Gazibegović-Busuladžić, D. B. Milošević, and W. Becker, J. Phys. B **41**, 201004 (2008).

[27] M. Meckel, D. Comtois, D. Zeidler, A. Staudte, D. Pavičić, H. C. Bandulet, H. Pépin, J. C. Kieffer, R. Dörner, D. M. Villeneuve, and P. B. Corkum, Science **320**, 1478 (2008).